

Iodine spectroscopy and absolute frequency stabilization with the second harmonic of the 1319-nm Nd:YAG laser

A. Arie,* M. L. Bortz, M. M. Fejer, and R. L. Byer

E. L. Ginzton Laboratory, Stanford University, Stanford, California 94305

Received June 9, 1993

We have frequency doubled a 1319-nm Nd:YAG laser in a quasi-phase-matched LiNbO₃ waveguide and used the ≈1-mW second-harmonic output to investigate the ¹²⁷I₂ transitions near 660 nm. We reached submegahertz laser-frequency stability at a (vacuum) wavelength of 1319.098 nm by locking the second harmonic to the center of the P(48)6-6 transition.

Absolute frequency stabilization of laser sources in the 1.3–1.55-μm range is required for frequency references in fiber-optic densely packed wavelength-multiplexed or coherent communication systems.^{1,2} Locking of both the transmitter and the local oscillator to absolute references may permit cold-start coherent communication,² saving the need to acquire and lock the local oscillator frequency to that of the transmitter. Absolutely stabilized sources can also be used for precision metrological measurements and fiber-optic sensing applications.³ The monolithic diode-pumped 1319-nm Nd:YAG laser is an attractive source for these applications because of its inherently narrow linewidth (<10 kHz in 1 ms), low-intensity noise (shot noise limited above 5 MHz), and relatively high power (>150 mW in a TEM₀₀ mode).⁴ Whereas semiconductor lasers in the 1.3-μm range have been absolutely stabilized with the optogalvanic effect in noble gases² and to transitions between excited states in optically pumped rubidium,⁵ none of these atomic transitions falls within the 0.7-nm-gain bandwidth of the Nd:YAG laser. Hydrogen fluoride molecules contain many absorption lines in the 1.3-μm range,⁶ but this material is highly corrosive. Nd:YAG lasers have been locked to Fabry–Perot cavities,⁷ but this provides only relative frequency stabilization and is sensitive to the long-term drift of the Fabry–Perot cavity.

Nonlinear optical-frequency conversion enables infrared sources to be locked to absorption lines in the visible. For example, second-harmonic generation (SHG) was used to frequency double 1064-nm Nd:YAG lasers and lock to Doppler-broadened⁸ and Doppler-free⁹ lines of iodine near 532 nm. However, achieving useful SHG conversion efficiencies with low-power cw lasers requires resonant frequency conversion.¹⁰ This requires a servo controller to lock the resonant frequency of the doubling cavity to the laser frequency,⁹ thus increasing experimental complexity. In this Letter we demonstrate efficient single-pass SHG of a 1319-nm Nd:YAG laser and absolute frequency stabilization by locking the second harmonic to molecular-iodine absorption lines near 660 nm.

High single-pass SHG conversion efficiencies may be achieved with quasi-phase-matched waveguide-frequency conversion. Quasi-phase matching (QPM)

permits phase-velocity matching by a periodic modulation in the material nonlinear coefficient.¹¹ In LiNbO₃ this technique is accomplished by periodic ferroelectric domain reversal and permits the use of the large d_{33} nonlinear coefficient, which is not accessible to birefringent phase matching. The improvement in conversion efficiency compared with that for the birefringent process is $(2d_{33}/\pi d_{31})^2 \approx 20$, where $2/\pi$ is the QPM reduction factor¹¹ and d_{31} is the birefringent nonlinear coefficient. QPM provides relaxed temperature and wavelength tolerances, because both the fundamental and the second harmonic are extraordinarily polarized, and permits room-temperature operation. QPM can be combined with waveguide confinement, thus providing a further increase in conversion efficiency, which scales as $\lambda_w L/A_{\text{eff}}$ over confocally focused bulk interactions, where λ_w is the laser wavelength, L is the phase-matched interaction length, and A_{eff} is the effective waveguide cross-sectional area. The combination of QPM and waveguide confinement can yield high single-pass conversion efficiencies.

The QPM waveguide-frequency doubler was fabricated by the formation of a ferroelectric domain grating on the surface of a LiNbO₃ wafer, followed by a channel waveguide parallel to the grating wave vector. The domain grating was fabricated with the titanium-indiffusion technique for ferroelectric domain inversion.¹² A 10-nm-thick, 10.5-μm period (3.5-μm lines) titanium grating was lithographically delineated on the +z surface of LiNbO₃ and diffused at 1100 °C for 10 min into the LiNbO₃ substrate. Channel waveguides were then formed with the annealed proton-exchange process,¹³ with an initial proton-exchange depth of 0.32 μm and an anneal time of 5 h at 333 °C. In a channel with a mask width of 5.75 μm the TM₀₀ modes at the Nd:YAG fundamental wavelength and its second harmonic were phase matched at ~35 °C. With the bulk LiNbO₃ refractive indices the FWHM temperature bandwidth of this interaction is estimated to be 44 °C mm and the wavelength bandwidth is 5.6 nm mm. Hence the 5-mm-long sample had a >8 °C temperature bandwidth that eliminated the need for precise temperature control and a wavelength bandwidth that exceeded the entire tuning range of the 1319-nm Nd:YAG laser transition. A monolithic Nd:YAG ring laser⁴

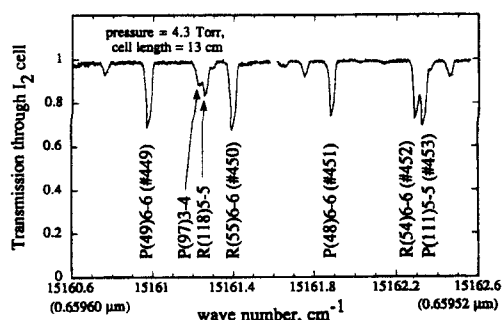


Fig. 1. Normalized transmission through the $^{127}\text{I}_2$ cell. Two separate scans were combined: the left part (15161.6 cm^{-1}) by scanning the laser temperature between 46 and 40°C , and the right part by scanning between 30 and 24°C . Line numbers are taken from Ref. 14.

emitting 160 mW of power at 1319 nm was used to pump the waveguide. More than 1 mW of second-harmonic power was generated with ≈ 100 mW of pump power coupled into the waveguide, exceeding the single-pass, birefringently phase-matched, confocally focused bulk conversion efficiency by a factor of ~ 170 .

The absorption lines of molecular $^{127}\text{I}_2$ were used as the frequency reference for the Nd:YAG laser stabilization. The thoroughly characterized¹⁴ spectrum of the $X \rightarrow B$ transitions in molecular iodine contains many absorption lines in the 500–700-nm range, and the molecular constants have been accurately determined.¹⁵ In addition, because I_2 was used to stabilize various visible lasers, the frequency offset mechanisms are well known and quantified. However, the weak absorption lines near 660 nm, originating from high vibrational levels in the ground (X) state, necessitate heating the 13-cm-long iodine cell to increase the vapor pressure. The cell windows were heated to a slightly higher temperature than the cell body to prevent iodine condensation on the windows, and the temperature (and pressure) of the cell cold point was monitored with a thermocouple. By ramping the laser temperature, we achieved a continuous frequency scan of 15 GHz (at 1319 nm) between mode hops.

Figure 1 shows the 10 observed iodine absorption lines. Five of these lines (449–453) are listed in the iodine atlas¹⁴ and have been identified with a wavemeter. Table 1 gives the assignments of the stronger iodine lines, determined by calculation of the wave numbers of the transitions that best match the results given in Ref. 14.¹⁵ The two strong lines between lines 449 and 450, which do not appear in the iodine atlas, have also been assigned. The accuracy of the calculated wavelengths¹⁵ is 2 parts in 10^7 , i.e., 91 MHz, or 0.00013 nm at 660 nm.

The monolithic ring laser had a continuous tuning range of -2.4 GHz/K between mode hops and the peak of the gain tuned by -1 GHz/K .⁴ As a result of this tuning behavior each absorption line was usually observed twice at two different crystal temperatures. For instance the $P(48)6-6$ line was observed at 28.6°C , but after a mode hop at 33.2°C . At the

center point between two mode hops the laser should oscillate near the peak of the gain curve. Using the I_2 absorption lines as wavelength markers, we determined the peak of the gain wavelength for our Nd:YAG laser to be $1319.080 \pm 0.01\text{ nm}$ at 27.1°C and $1319.166 \pm 0.01\text{ nm}$ at 42.6°C .

Figure 2 shows the experimental setup for frequency locking the laser to iodine. The $P(48)6-6$ transition (line 451) was used as a frequency reference. The Doppler broadening of $^{127}\text{I}_2$ at 660 nm is $\sim 350\text{ MHz}$, but the splitting of this line into 15 hyperfine transitions⁸ results in a measured linewidth of $\sim 800\text{ MHz}$. The peak absorption for this line was measured at four different cell temperatures between 40 and 70°C , and the normalized absorption coefficient was calculated as $0.56\text{ m}^{-1}\text{ Torr}^{-1}$. We used FM spectroscopy to obtain an error signal to lock to I_2 transitions. The second-harmonic light was frequency modulated at 105 MHz with an electro-optic phase modulator with a modulation coefficient of ~ 0.3 and was passed through a 13-cm I_2 cell held at a temperature of 57°C (pressure $\sim 3.5\text{ Torr}$). The detected signal was mixed with a local oscillator after an appropriate phase delay and fed through a servo amplifier to the piezofrequency actuator of the laser, thereby locking the laser frequency to the zero crossing point of the FM signal. Using the calculated wavelength of the $P(48)6-6$ transition given in Table 1, we determined the wavelength of the locked laser to be 1319.098 nm (7580.940 cm^{-1}). To evaluate the frequency stability, we used a second 15-cm I_2 cell held at 38.5°C (pressure $\sim 0.9\text{ Torr}$). This independent monitoring of the stability was required for observation of frequency fluctuations caused by servo electronics and the cell used for locking, which

Table 1. $^{127}\text{I}_2$ Absorption Lines within the Tuning Range of the Frequency-Doubled 1319-nm Nd:YAG Laser

Line No.	Measured (cm^{-1}) ^a	Calculated (cm^{-1}) ^a	Assignment
449	15 160.978 8	15 160.976 2	$P(49)6-6$
		15 161.229 5	$P(97)3-4$
		15 161.259 0	$R(118)5-5$
450	15 161.395 0	15 161.392 7	$R(55)6-6$
451	15 161.881 3	15 161.879 6	$P(48)6-6$
452	15 162.288 0	15 162.288 8	$R(54)6-6$
453	15 162.323 7	15 162.326 3	$P(111)5-5$

^aRef. 14.

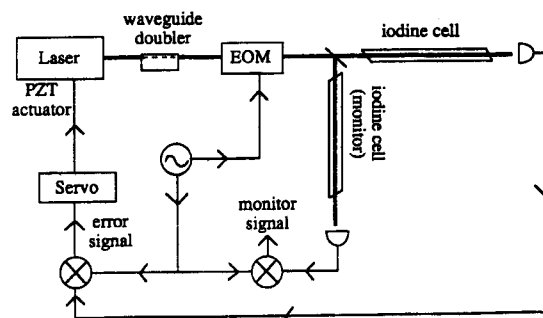


Fig. 2. Experimental setup for locking the laser to I_2 lines. EOM, electro-optic modulator; PZT, piezoelectric.

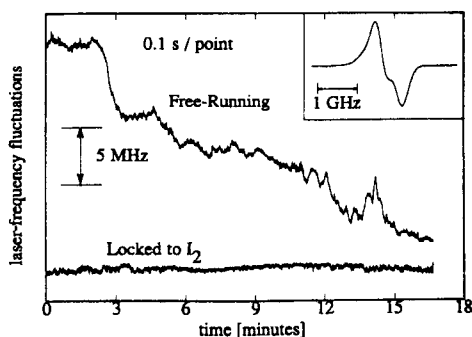


Fig. 3. Typical variations of laser frequency, measured with an independent (monitor) I_2 cell, under free-running and I_2 -locked conditions. The inset shows the FM error signal of the $P(48)6-6$ line.

cannot be detected by direct measurement of the closed-loop error signal.

Figure 3 shows typical laser fluctuations under free-running and I_2 -locked conditions. Each graph contains a set of 10,000 successive measurements, with 0.1 s per measurement point. Whereas the free-running laser drifted by 18.6 MHz during the 16.5 min of measurement, the stabilized laser fluctuations remained at the submegahertz level. The standard deviation of the frequency fluctuation was 210.6 kHz, and the two-sample frequency deviation was 55.1 kHz; hence normalizing by the laser frequency (227 THz) yielded a root Allan variance of 2.4×10^{-10} . The maximum frequency excursion during this measurement was 1.06 MHz. The laser remained locked as long as the frequency drift did not exceed the piezoactuator range, typically >1 h. An additional servo, connected to the temperature frequency actuator of the laser, could keep the laser locked indefinitely.

With 150 μ W of power falling on each detector the dominant noise was the thermal and amplifier noise of the detection systems. Long-term frequency fluctuations of the locked laser were dominated by variation in the radio-frequency pickup level. Further improvements are possible by use of a ~ 1 -GHz phase modulator with optimal modulation coefficient⁷ of 1.08 and by amplification of the detected signal with a low-noise-resonant transimpedance amplifier. An alternative and simpler method of frequency stabilization can be achieved by locking to the 50% transmission point on one side of the Doppler-broadened line. However, this technique can be used only if larger frequency excursions are tolerated, because of higher sensitivity to variations in laser power and cell absorption. Significantly better frequency stability and reproducibility by locking to the Doppler-free lines⁹ of iodine may require higher second-harmonic power levels. Second-harmonic conversion efficiencies approaching 100% W^{-1} can be achieved by increasing the waveguide length and optimizing the waveguide dimensions. Frequency stabilization of other solid-state and semiconductor sources in the 1.3–1.55- μ m range may be achieved with efficient waveguide SHG. Additional frequency references for the second harmonic include absorption lines in water and

the atomic absorption lines of rubidium at 780 nm (Ref. 16) or calcium at 657 nm. Finally, integration of phase and amplitude modulators and directional couplers along with the waveguide-frequency doubler should be straightforward because of the well-established integrated-optics technologies in $LiNbO_3$.

In summary, we have absolutely stabilized the 1319-nm Nd:YAG laser by locking its second harmonic to absorption lines of I_2 and improved the long-term frequency stability and reproducibility of this laser. Our locking scheme used an external phase modulator; hence there was no need to dither the laser frequency. Frequency fluctuations of the locked laser are at the submegahertz level for an integration time of 0.1 s, whereas we observed daily fluctuations of several hundred megahertz for a free-running laser. An important feature for precision metrological measurement is that two stabilized harmonically related wavelengths are available. The high single-pass conversion efficiency of the quasi-phase-matched waveguide-frequency doubler, combined with thoroughly characterized molecular and atomic absorbers in the visible and near-infrared spectral range, offers an alternative method of wavelength and frequency control in advanced multiple-wavelength optical communication systems.

*Present address, Faculty of Engineering, Tel Aviv University, Ramat Aviv, Tel Aviv 69978, Israel.

References

1. Y. Sakai, S. Sudo, and T. Ikegami, *IEEE J. Quantum Electron.* **28**, 75 (1992).
2. Y. C. Chung, *J. Lightwave Technol.* **8**, 869 (1990).
3. D. J. Webb, J. D. C. Jones, and D. A. Jackson, *Electron. Lett.* **24**, 1002 (1988).
4. Specifications of the 122-1319-150 laser, Lightwave Electronics, 1161 San Antonio Road, Mountain View, Calif. 94043.
5. R. Boucher, M. Breton, N. Cyr, and M. Tetu, *IEEE Photon. Technol. Lett.* **4**, 327 (1992).
6. S. Yamaguchi and M. Suzuki, *Appl. Phys. Lett.* **41**, 1034 (1982).
7. F. Zhou and A. I. Ferguson, *Opt. Lett.* **16**, 79 (1991); T. Day, E. K. Gustafson, and R. L. Byer, *IEEE J. Quantum Electron.* **28**, 1106 (1992).
8. A. Arie and R. L. Byer, "Frequency stabilization of the 1064-nm Nd:YAG lasers to Doppler-broadened lines of iodine," *Appl. Opt.* (to be published).
9. A. Arie, S. Schiller, E. K. Gustafson, and R. L. Byer, *Opt. Lett.* **17**, 1204 (1992).
10. W. J. Kozlovsky, C. D. Nabors, and R. L. Byer, *IEEE J. Quantum Electron.* **24**, 913 (1988).
11. J. A. Armstrong, N. Blombergen, J. Ducuing, and P. S. Pershan, *Phys. Rev.* **127**, 1918 (1962).
12. E. J. Lim, M. M. Fejer, R. L. Byer, and W. J. Kozlovsky, *Electron. Lett.* **25**, 731 (1989).
13. P. G. Suchoski, T. K. Findakly, and F. J. Leonberger, *Opt. Lett.* **13**, 1050 (1988).
14. S. Gerstenkorn and P. Luc, *Atlas Du Spectre D'Absorption de la Molecule D'Iode* (Editions du CNRS, Paris, 1978).
15. S. Gerstenkorn and P. Luc, *J. Phys. (Paris)* **46**, 867 (1985).
16. M. Ohtsu and E. Ikegami, *Electron. Lett.* **25**, 22 (1989).